Microstructures and tribological properties of ferrous coatings deposited by APS (Atmospheric Plasma Spraying) on Al-alloy substrate

Aleksandar Vencl
Research and Teaching Assistant
University of Belgrade
Faculty of Mechanical Engineering

Mihailo Mrdak
Research Guide
Aeronautical Plant "Moma Stanojlović"

Ivana Cvijović
Research Assistant
Institute of Nuclear Sciences "Vinča"

Using of Al-alloys for producing of engine blocks in automotive industry results in weight savings and lower fuel consumption and therefore reduced pollution. Thermal spray coatings are one of the solutions for improving poor tribological properties of aluminium. In this paper, the microstructures and tribological properties of two types of ferrous thermal spray coatings were analysed and compared with gray cast iron as a standard material for cylinder blocks. Process used for coating deposition on Al-Si alloy substrate was Atmospheric Plasma Spraying (APS). The pin-on-ring tribometer was used to carry out these tests under lubricated sliding conditions, sliding speed of 0.5 m/s*, sliding distance of* 5000 m *and normal load of* 450 N*. Tribological test results showed that, for the investigated conditions both coatings had satisfactory values of wear and friction and that they could be adequate substitution for gray cast iron as a material for cylinder blocks.*

Keywords: *Atmospheric plasma spraying, ferrous coatings, microstructure, sliding wear, friction.*

1. INTRODUCTION

Aluminium alloys have attractive physical and mechanical properties. They are lightweight, low costs production (with sand casting technology), easy to machine and have good recycling possibilities (up to 95 %) [1]. Due to these facts, their application in automotive and other industries is increasing. One of the applications in automotive industry is replacing of material for engine blocks, which has been traditionally made entirely of gray cast iron. Today, more than 60 % of the engines for passenger cars are produced in cast aluminium alloys [2] with some concrete examples [3]. This change is brought by the need to reduce vehicle weight in order to improve fuel economy.

Unfortunately tribological properties of pure and unprotected aluminium are poor comparing with gray cast iron. There is more than one solution for that problem. Currently, as one of the solutions, cast iron liners are used to obviate these problems. Use of cast iron liners, because of their good operating characteristics, is not the best solution. These liners need to have a specific wall thickness, which results in a relatively large web width between the individual cylinder bores and increases the dimensions and weight of the engine. Removing the need for liners, the engine length can be significantly reduced and weight savings of more than 1 kg per engine can be achieved [4].

Another solution is to provide protection of aluminium alloy, and chemical and thermal spray coatings are most predominant surface treatments. At present, chemical treatments like electroplating of chromium and nickel coatings are becoming increasingly threatened by environmental regulation. Moreover, one should prevent microscopic particles of chromium and nickel, a health hazard, from entering the environment through the exhaust pipe. This process requires complex chemistry and is relatively expensive. Thermal spray coatings are a relatively new solution for cylinder bore protection and plasma spray process is the only industrially commercialised one. Comparisons of these two solutions as well as use of cast iron liner was done by Sulzer Metco company, with results that show better characteristic of plasma coatings in all test criteria's [5].

In this paper, the microstructures and compositions and of two types of ferrous thermal spray coatings, deposited on Al-alloy substrate using an APS (Atmospheric Plasma Spraying) process, were analysed. Their tribological properties were compared with gray cast iron as a standard material for cylinder blocks.

2. THERMAL SPRAY PROCESS

Advantage of thermal spray process, compared to the other coating processes, is that it has a great range of coating materials, coating thickness and possible coating characteristics.

Received: February 2006, Accepted: May 2006
Correspondence to: Aleksandar Vencl
Faculty of Mechanical Engineering,
Kraljice Marije 16, 11120 Belgrade 35, Serbia
E-mail: avencl@mas.bg.ac.yu

2.1 Principle of thermal spray process

During the thermal spraying process, melted or molten spray material is propelled, by process gases, onto a cleaned and prepared component surface. The liquid or molten coating particles impact the surface at high speed. This causes the particles to deform into splats and spread like "pancakes" on the substrate (Fig. 1). Heat from the hot particles is transferred to the cooler base material. As the particles shrink and solidify, they bond to the roughened base material. Adhesion of the coating is therefore based on mechanical "hooking". Because the adhesion of the coating to the substrate predominantly consists of mechanical bonding, pretreatment of the surface is very important. The surface of the substrate is usually roughened and activated, so the area for bonding of the sprayed particles is increased. The thickness of the sprayed coating is normally between approximately 50 μm and a few mm. The thermal energy used to melt the coating material, may be generally divided into two categories: electrical and flame heating.

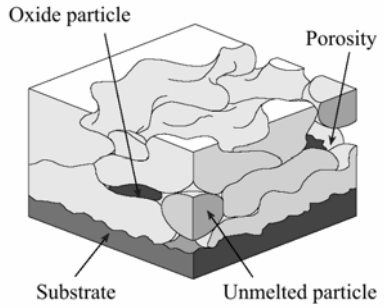

Figure 1. Schematic diagram of a thermal sprayed coating

There are several different processes for thermal spray coating deposition and mostly used are [6-9]:

- Conventional flame spray (wire and powder flame spray),
- Electric arc wire spray,
- Plasma spray (atmospheric and vacuum plasma spraying), and
- High velocity oxy-fuel spray (HVOF).

Description and comparison of these processes can be found elsewhere [9-11]. Process used in this investigation is atmospheric plasma spraying.

2.2 Atmospheric plasma spraying (APS)

In the plasma spraying process (Fig. 2), the thermal energy of a high frequency electric arc (ignited between water-cooled anode and cathode) together with a plasma forming gas (flowing through between the electrodes), is utilized in the melting and projecting of the deposit material at high velocities (300-600 m/s), onto a substrate. A plasma gas (Ar, He, H_2, N_2 or mixtures) is introduced at the back of the gun interior.

The main use of this system is to generate high temperatures, reaching up to 16,000°C, for the deposition of materials with high melting temperatures. The deposit material is generally in powder form and requires a carrier gas to feed the powder into the plasma flame.

Vacuum plasma spraying (VPS) is a variant of the process where plasma spraying is in a controlled, low pressure atmosphere, resulting in coatings with less oxides.

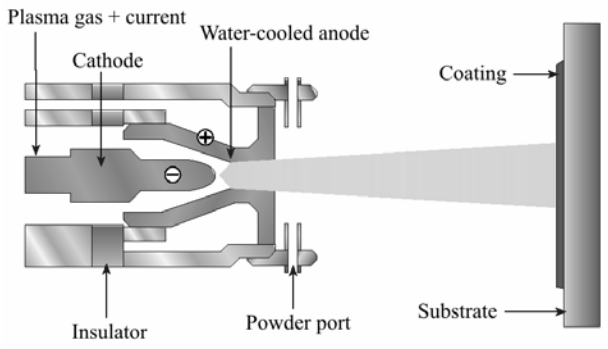

Figure 2. Schematic diagram of the plasma spray process

2.3 Coating Characterization

Depending on the application of the coating, different characteristics are important but there are some characteristics which are the same for all applications: coating thickness, porosity, structure, presence of unmelted particles and oxide inclusions, microhardness and bond strength. Coating characteristics are very dependent on spray parameters. According to some researchers [12], there are more than 50 macroscopic parameters that influence the quality of the coating and the production of coating is still based on trial and error approach.

The resultant coating is a composite of the alloy with oxides formed during deposition. Presence of the FeO (wustite) and Fe_3O_4 (magnetite) oxides, as solid lubricants, improves the tribological properties of the coating. The formation of Fe_2O_3 (hematite) oxide should be avoided, because it is abrasive. The residual porosity of the plasma coating should help to reduce the coefficient of friction through a micro-cavity lubrication system, where micro-cavity serves as a lubricant reservoir allowing improved lubrication process.

3. EXPERIMENTAL DETAILS

3.1 Material

Substrate material was a Al-Si alloy (EN AlSi10Mg), referred as L21. The chemical composition was: Al-9.8Si-0.48Fe-0.1Cu-0.2Mn-0.3Mg-0.08Zn-0.05Ti (wt.%) and it was fabricated using sand casting, followed with solution annealing at 540°C with 35°C/h, water quenching and artificial ageing at 160±5°C for 6 h.

Two spray powders were used in this experiment, referred to as "A" and "B". The chemical compositions of the powders are shown in Table 1. The powder size was: less than 50 μm and less than 38 μm in diameter for powder "A" and "B", respectively (Fig. 3).

A gray cast iron (ref. as SL 26) was chosen as a standard material to compare its performances with the coatings. The chemical composition of this material, fabricated using the sand casting procedure followed by heating at 550°C in order to eliminate residual stress in the material, is shown in Table 1.

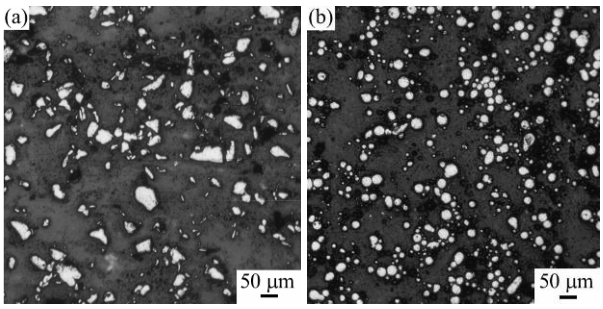

Figure 3. OM micrograph of (a) A and (b) B powder

Table 1. Chemical composition of used powders and gray cast iron SL 26

Powder / material	Element, wt. %						
	C	Si	Mn	P	Cr	Ni	Fe
A	3.5	-	0.35	-	-	-	Balance
B	1.2		1.5		1.3	0.3	Balance
SL 26	3.18	2.17	0.60	0.7	0.37	-	Balance

3.2 Spray conditions

Atmospheric Plasma Spraying (APS), with METCO 7MB Plasma Flame Spray Gun, was utilized in the experiment. Before the spraying process, surface of the aluminium alloy substrate was roughened with brown fused alumina (Al_2O_3) using particle sizes of 106–125 μm. The target coating thickness was 200–300 μm, and the spray conditions are shown in Table 2.

Table 2. APS condition for used powders

Spray parameters	A	B
Argon, l/min	80	100
Hydrogen, l/min	15	5
Current, A	500	500
Argon powder gas, l/min	37	37
Powder feed rate, kg/h	4.5	2
Spray distance, mm	75	150

3.3 Microstructure analysis and hardness tests

The microstructure of test materials was analysed by optical microscope (OM), where the coatings were sectioned perpendicular to the coated surface. Phases present in the coatings were analysed by X-ray diffraction (XRD). After the identification of oxides, their volume fraction, as well as porosity, presence of cracks and unmelted particles, were measured by image analysis on higher-magnification OM micrographs. Characterisation was done according to the Pratt & Whitney standard practices manual. Hardness was measured using a Vickers hardness tester under a 10 kg load, and the microhardness was measured under a 100 g load using a micro-Vickers hardness tester.

3.4 Tribological testing

Tribological tests were carried out on the pin-on-ring tribometer under lubricated sliding conditions, in ambient air at room temperature (≈ 25°C). A schematic diagram of tribometer is presented in Figure 4. Cylindrical pins of tested materials having 10 mm diameter and 15 mm length were used as wear test samples. Ring (hereafter referred to as counter body) of 50 mm diameter and 10 mm thickness was made of nodular gray cast iron (ref. as NL-1). This material was chosen as a standard piston ring material with specification according to the ISO standard (Subclass Code MC 53) [13].

Lubrication was provided by revolving of the ring which was sunk into oil container. Lubricant was mineral engine oil (SAE 15W-40, ACEA E3).

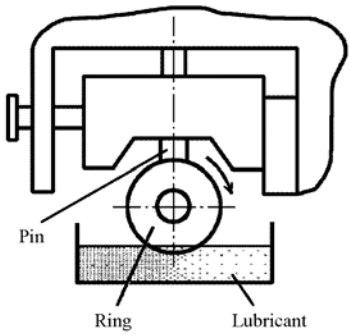

Figure 4. Schematic diagram of the pin-on-ring tribometer

Before and after testing, both the pin and the counter body (ring) were degreased and cleaned with benzine. Wear scars on pins were measured in accordance with ASTM G77 [14] with accuracy of 0.05 mm, after each test to calculate the volume loss. The values of oil temperature, friction coefficient, normal and friction force were monitored during the test and through data acquisition system stored in the PC.

Tests were carried out at selected test conditions: sliding speed of 0.5 m/s, sliding distance of 5000 m and normal load of 450 N.

Surface roughness of test specimens was $Ra = 0.3 - 0.4$ μm .

After testing, worn surfaces of pins were examined by optical microscopy.

4. RESULTS AND DISCUSSION

4.1 Microstructure, coating thickness and hardness

Microstructure of L21 alloy (Fig. 5a) consists of eutectic particles and dendrites of α solid solution. Porosity was not detected in the microstructure.

Graphite nodules and some carbide particles can be distinguished in improved NL-1 alloy microstructure (Fig. 5b).

Microstructure of the cast SL 26 alloy consists of phosphide eutectic and graphite flakes in the fine perlite matrix, as shown in Figure 6. Graphite flakes, No. 4-6 in size, conformed to the type A and B morphologies.

The microstructures of two types of coatings are shown in Figures 7 and 8. In both coatings, elongated splats of molten powder form a lamellar structure, with oxide layers in between, typical for spray coatings [15-17].

No cracking was found in the coatings and no peeling was observed at the interface between the coating and the substrate (Fig. 7). A cross-section of the coatings at higher magnification is shown in Figure 7. Oxide content for coating A was approximately 13% and for coating B was around 41%. Porosity in the A and B coatings was 2.3% and 5.8%, respectively.

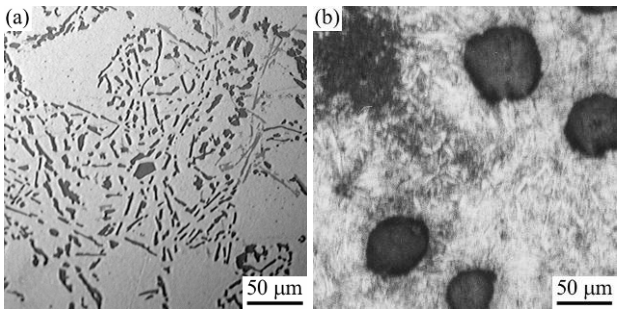

Figure 5. OM microphotograph of (a) L21 and (b) NL-1 microstructure

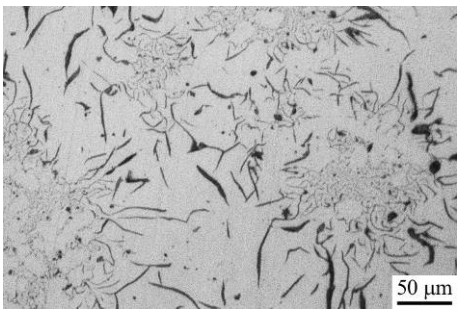

Figure 6. OM microphotograph of SL 26 microstructure

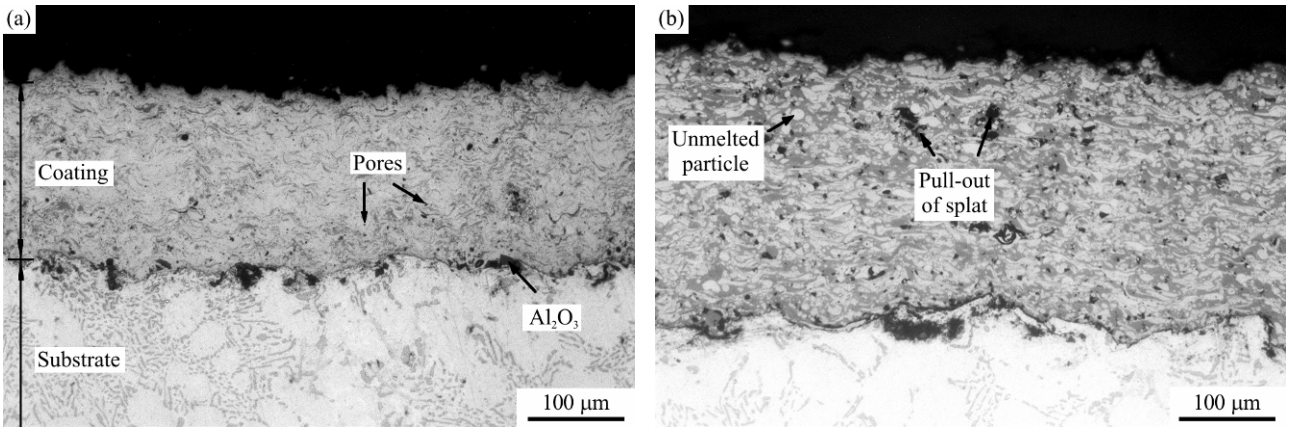

Figure 7. OM micrograph of (a) A and (b) B coating

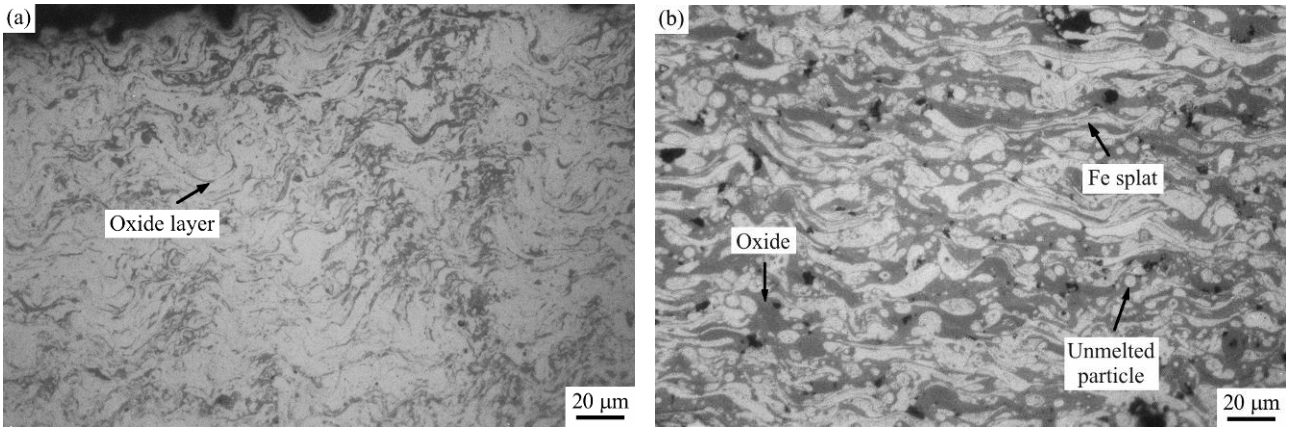

Figure 8. Higher magnification OM cross-section micrograph of (a) A and (b) B coating

Big dark area, indicated with arrows, could be pull-outs of splats or dirt formed during polishing.

Volume fraction of unmelted particles in the coating B is approximately 10 %, while unmelted particles were not detected in coating A. It must be mentioned that porosity of the coating B was detected in areas with unmelted particles (Fig. 8).

X-ray diffraction (XRD) analysis revealed that A coating structure consists of elemental iron (Fe) and magnetite (Fe_3O_4), while B coating contains elemental iron (Fe) and wustite (FeO). The other phases are present in a small amount, less than 3% (Fig. 9).

Coating thickness before machining was 200 μm and 270 μm for coating A and B, respectively. With machining, 100 μm of coating thickness was removed. The distribution of coating thicknesses can be considered to be very stable.

Hardness of tested materials is shown in Table 3.

Table 3. Hardness of tested materials

Material	Hardness, HV 10	Microhardness, HV 0.1
L21	51.95	96
SL 26	254	329
A	-	506
B	-	433
NL-1	220	238

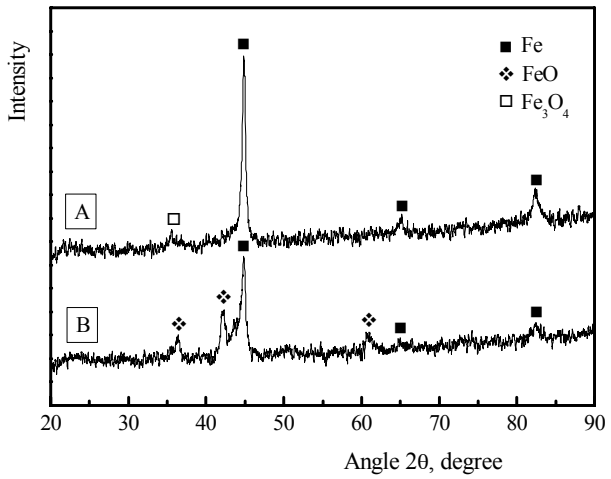

Figure 9. XRD patterns of tested coatings

4.2 Tribological properties

Tribological investigation of these coatings was just an initial one, with preliminary results and some more experiments to be done to completely understand tribological behaviour of ferrous coatings deposited by APS on Al-alloy substrate.

In order to achieve a higher confidence level in evaluating test results, five replicate tests were run for all the tested materials. The results indicate good reproducibility of the wear and friction results.

Wear and friction test results showed that for the investigated conditions SL 26 and coating A had very similar values (Fig. 10). Coating B had inferior values, but not in a way that it couldn't be, as well as coating A, adequate substitution for gray cast iron as a material for cylinder blocks.

Lubricant temperature was rising during the tests, since it was not controlled, but after initial running-in period it became stable and had the value of 56 - 58 °C.

The values of final dynamic coefficient of friction indicates boundary lubrication condition and these values are in correlation with wear characteristic. Both values were the highest with coating B, then they decreased with SL 26 and were the smallest with coating A.

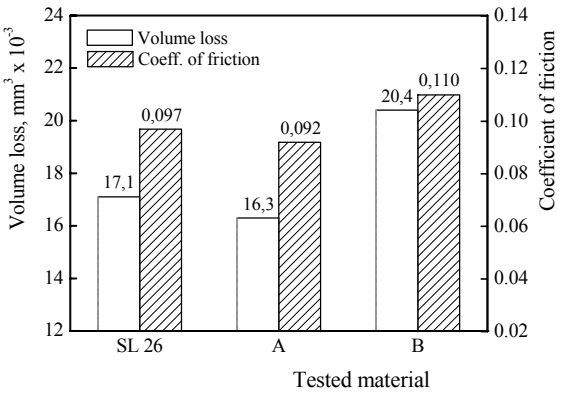

Figure 10. Volume losses and coefficient of friction for tested materials

Wear values are in partial correlation with hardness values. They should decrease as hardness increases, and that happens with coatings, since A coating was harder than B coating. For SL 26 wear values should not been viewed only as a function of hardness, yet a presence of graphite as a solid lubricant should be also considered. High presence of oxides in the coatings could have influence on their wear values. Oxides are harder than Fe splats matrix and when the difference is too large, cracks are initiated at oxides and at oxides/matrix interfaces (pre-existing pores and cracks play a similar role), and parts of oxides are fallen off as wear proceeds, causing large protuberances on the worn surface [18]. Low fracture toughness of the interfacial oxide could also cause splat delamination upon frictional contact [20]. It is possible that unmelted particles were also fallen off and caused heavier wear at B coating than at A coating, since it was more present in coating B.

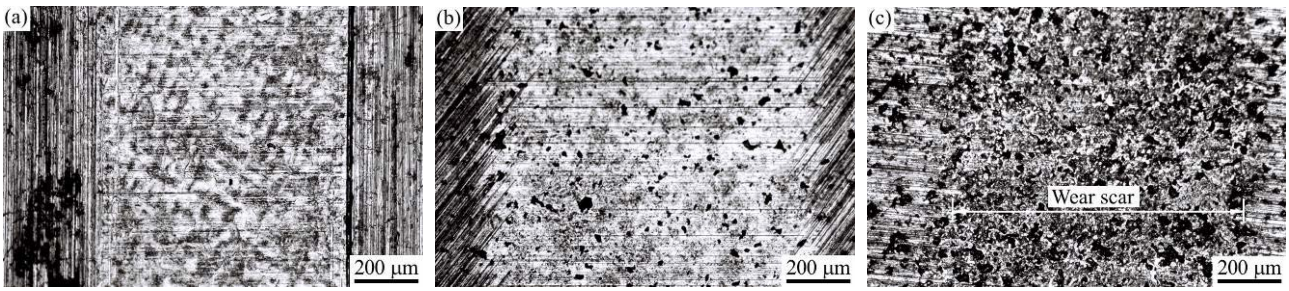

Figure 11. OM micrographs of pin wear scars for (a) SL 26, (b) A and (c) B samples

Figure 12. OM micrographs, at higher magnification, of pin worn surfaces for (a) SL 26, (b) A and (c) B samples

OM micrographs of worn surfaces for tested materials are shown in Figures 11 and 12. Higher presence of oxides in the coating B compared to the coating A is obvious. Oxides are darker and profounder than Fe splats which were polished during sliding. Scratches on the metal splats are from abrasive wear.

The wear test data did not comprise wear values of the counterpart, which is necessary to achieve optimal operating condition of the system and required service life.

This study has presented the possibility that wear-resistant ferrous coatings tested here can actually be applied to engine cylinder bores by discussing some factors affecting the wear of the coating in relation with the microstructure. To further improve the ferrous coatings, understanding of the wear behaviour occurring under various loads and speeds is required, in order to establish optimal spraying methods and conditions. Wear values of the coating and the counterpart material should be also considered simultaneously to enhance the overall wear properties of the ferrous coatings.

5. CONCLUSION

Two kinds of ferrous coated layers were deposited on Al-alloy substrate, by atmospheric plasma spraying, and their microstructure and tribological properties were investigated with the following conclusions.

Microstructural analysis of the coatings showed lamellar structure with elongated splats of molten powder and formation of iron oxides in between, as a result of the reaction with oxygen in the air. Presence of pores and unmelted particles was also noticed.

X-ray diffraction analysis revealed presence of two iron oxides: magnetite (Fe_3O_4) in coating A and wustite (FeO) in coating B.

Hardness of A coating was higher than of B coating and that had great influence on their tribological properties.

Tribological test results showed that for the investigated conditions both coatings could be adequate substitution for gray cast iron as a standard material for cylinder blocks. Research carried out until now indicates that from technical aspects ferrous coating deposited by atmospheric plasma spray process is one of the possible solutions for tribological problems of engine blocks made of aluminium alloys.

ACKNOWLEDGEMENTS

This work has been performed under the EUREKA programme project E! 3240. Help from the partners of the project (Petar Drapšin, Serbia, for providing and preparing the test specimens) as well as financial support received from Republic of Serbia, Ministry of Science and Environmental Protection, are gratefully acknowledged.

REFERENCES

[1] http://www.eaa.net/downloads/auto.pdf - Aluminium in Automotive Industry, European Aluminium Association, Brochure.

[2] Barbezat, G.: Advanced thermal spray technology and coating for lightweight engine blocks for the automotive industry, Surface & Coatings Technology, Vol. 200, No. 5-6, pp. 1990–1993, 2005.

[3] http//www.autoaluminum.org/engines.htm

[4] http//www.sulzermetaplas.com/map/SulzerDocuments/DocumentsImages/MetcoTechnicalPapers/smtech18.pdf - Harrison, K.: Improved Performance in Car Engines through Plasma Sprayed Coatings, Sulzer Metco Technical Paper

[5] http://www.sulzermetco.com/eprise/Sulzermetco/Sites/MetaNavigation/IndustrySolutions/AutoSolutions/case1.html - *Automotive Solution Kit*, Sulzer Metco, Brochure

[6] Tanner, B.: *Thermal Spray*, Sulzer Metco, 2004.

[7] Stachowiak, G.W., Batchelor, A.W.: *Engineering Tribology*, Butterworth-Heinemann, 2000.

[8] Andersson, P., Tamminen, J., Sandström, C.E.: *Piston ring tribology, A literature survey*, VTT Research Notes 2178, VTT, Finland, 2002.

[9] http://webpages.dcu.ie/~stokesjt/ThermalSpraying/Book/HVOFThermalSpraying.htm - Stokes, J.: *The Theory and Application of the HVOF Thermal Spray Process*, 2003.

[10] Barbezat, G.: The State of the Art of the Internal Plasma Spraying on Cylinder Bore in AlSi Cast Alloys, International Journal of Automotive Technology, Vol. 2, No. 2, pp. 47-52, 2001.

[11] Meyer, P., Rusch, W.: Production Coating Cost Comparison, in: Marple, B.R. and Moreau, C. (Ed.): *Thermal Spray 2003: Advancing the Science and Applying the Technology*, ASM International, pp. 123-128, 2003.

[12] Lugscheider, E., Barimani, C., Eckert, P., Eritt, U.: Modeling of the APS plasma spray process, Computational Materials Science, Vol. 7, No. 1-2, pp. 109-114, 1996.

[13] ISO 6621-3:2000 *Internal combustion engines - Piston rings* - Part 3: Material specifications, 2000.

[14] ASTM G77-98 Standard Test Method for Ranking Resistance of Materials to Sliding Wear Using Block-on-Ring Wear Test, Annual Book of ASTM Standards, Vol. 03.02, pp. 330-343, 2001.

[15] Schorr, B.S., Stein, K.J., Marder, A.R.: Characterization of Thermal Spray Coatings, Materials Characterization, Vol. 42, No. 2-3, pp. 93-100, 1999.

[16] Hwang, B., Ahn, J. and Lee, S.: Correlation of Microstructure and Wear Resistance of Ferrous Coatings Fabricated by Atmospheric Plasma Spraying, Metallurgical and Materials Transactions A, Vol. 33A, No. 9, pp. 2933-2945, 2002.

[17] Edrisy, A., Perry, T., Cheng, Y.T., Alpas, A.T.: The effect of humidity on the sliding wear of plasma transfer wire arc thermal sprayed low carbon steel coatings, Surface and Coatings Technology, Vol. 146-147, pp. 571–577, 2001.

[18] Hwang, B., Lee, S., Ahn, J.: Effect of oxides on wear resistance and surface roughness of ferrous coated layers fabricated by atmospheric plasma spraying, Materials Science and Engineering A, Vol. 335, No. 1-2, pp. 268–280, 2002.

[19] Rabiei, A., Mumm, D.R., Hutchinson, J.W., Schweinfest, R., Rühle, M., Evans, A.G.: Microstructure, deformation and cracking characteristics of thermal spray ferrous coatings, Materials Science and Engineering A, Vol. 269, No. 1-2, pp. 152–165, 1999.

МИКРОСТРУКТУРА И ТРИБОЛОШКЕ КАРАКТЕРИСТИКЕ ПРЕВЛАКА НА БАЗИ ГВОЖЂА НАНЕТИХ НА ОСНОВУ ОД Al ЛЕГУРЕ ПЛАЗМА СПРЕЈ ПОСТУПКОМ У АТМОСФЕРСКИМ УСЛОВИМА

Александар Венцл, Михаило Мрдак, Ивана Цвијовић

Коришћење легура алуминијума за израду блокова мотора у аутомобилској индустрији резултира смањењем тежине и уштедама у потрошњи горива, а самим тим и смањењем загађења околине. Превлаке нанете термички, процесом распршивања су једно од решења за побољшање, иначе лоших, триболошких карактеристика алуминијума. У овом раду су анализирани микроструктура и триболошке карактеристике два типа превлака на бази гвожђа и упоређене су са карактеристикама сивог лива као стандардног материјала за израду цилиндарских кошуљица. Превлаке су нанете на основу од Al-Si легуре плазма спреј поступком у атмосферским условима. За испитивања је коришћен трибометар типа “епрувета на прстену” у условима клизања са подмазивањем, при брзини клизања од 0,5 m/s, пређеном путу од 5000 m и нормалном оптерећењу од 450 N. Резултати триболошких испитивања показују да, за дате услове испитивања, обе превлаке имају задовољавајуће вредности хабања и трења и да могу бити адекватна замена за сиви лив као материјал за израду цилиндарских кошуљица.